Modeling of interfacial dynamic slip pulses with slip-weakening friction

Shiro Hirano and Teruo Yamashita[†]

Dynamic slip pulse propagation along a material interface is of great interest because many faults are known to lie along material interfaces and such interfaces may cause pulse-like ruptures. This subject has been extensively studied numerically over the last two decades. It has not, however, been studied very thoroughly from an analytical standpoint, although analytical studies would complement numerical ones. In particular, an analytical solution for removing stress singularities has not yet been obtained, even after an asymptotic analysis. In this paper, we employ three physically plausible conditions in our theoretical modeling: 1) arbitrary propagation speeds in the sub-Rayleigh range, 2) a slip-weakening friction law, and 3) boundedness of stress. We can construct an analytical solution under these conditions, and as a result of our parameter study, we determine the dependence of slip-weakening distance and the ratio of process zone size to pulse length on rupture direction and velocity. These results enable us to discuss a mechanism for limiting rupture velocity and estimating the slip-weakening distance in seismic inversion analyses.

1. Introduction

The observational study of Heaton [1990] has suggested that coseismic slip velocity for many earthquakes seems to be localized only near the rupture front and has significantly shorter duration than what is expected from classical crack models. This phenomenon, called the slip pulse, has interested many seismologists and its nature has been investigated widely. Theoretically, the slip pulse itself can be generated by various mechanisms: rate- or rate-and-state-dependent friction laws [e.g., Zheng & Rice 1998; Ampuero & Ben-Zion 2008; Noda et al. 2009], re-strengthening of the nucleation region [e.g., Nielsen & Madariaga 2003; Shi & Ben-Zion 2006], interaction between frictional heating and pore pressure changes [e.g., Suzuki & Yamashita 2008; Garagash 2012], 3-D effects of faults with large aspect ratios [e.g., Day 1982; Nakamura & Miyatake 2000; Dalguar & Day 2009], or rupture propagation along a material interface between dissimilar media, which will be detailed further in this section. It has also been pointed out that,

Department of Physical Science, College of Science and Engineering, Ritsumeikan University, 525-0058 Shiga, Japan. See https://interfacial.jp/ for contact details.
[†]Earthquake Research Institute, University of Tokyo, 113-0032 Tokyo, Japan.

theoretically, the sustained propagation of a slip pulse can be modeled on the assumption of a slip-weakening friction law as long as the value of the stress ratio S, defined as the ratio of strength excess to the stress drop, is in a certain range [e.g., Andrews 1976; Rice et al. 2005; Shi & Ben-Zion 2006]. Andrews [1976] performed numerical simulations for spontaneous mode II rupture growth only within the range $0.5 \leq S \leq 1$ and obtained no slip pulses but rather self-similar crack solutions. Rice et al. [2005], on the other hand, showed analytically that a steady-state slip pulse solution can exist for both mode II and mode III ruptures if $S \geq 2$ and friction weakening distance takes a specific value depending on the value of S. Sustainability of such a pulse was verified numerically by Shi & Ben-Zion [2006]. In this paper, we focus on slip pulse propagation in a steady-state analysis assuming a slip-weakening friction law. Such an analysis will be valid approximately when the rupture velocity and slip velocity do not oscillate violently but show small perturbations around mean values; such rupture behavior has been reported in some observational studies of source processes by using high-frequency components [e.g., Ishii et al. 2005; Okuwaki et al. 2014]. Moreover, steady-state analysis also has potential significance in understanding the sustainability of slip pulse propagation [Rice et al. 2005].

Although Rice et al. [2005] focused on slip pulse propagation in a homogeneous medium, major faults often lie along the interface of two different masses of rock with different origins, e.g., at plate interfaces or tectonic lines. Hence, the process of an earthquake therein could be modeled well as dynamic shear rupturing of the interface between two welded dissimilar elastic media, referred to as a bimaterial interface. Even if the bimaterial interface is assumed to be planar, inevitably there exist qualitatively different types of mode II rupture along the interface: one is rupture towards the slip direction of a relatively compliant medium, referred to as the "positive direction", and the other is rupture towards the slip direction of a relatively stiff medium, referred to as the "negative direction". Weertman [1963; 1969; 1980] mathematically analyzed steady-state propagation of a given in-plane slip velocity distribution along a bimaterial interface and found that, unlike the case of a homogeneous medium, propagation causes not only shear stress fluctuation over the entire interface but also normal stress fluctuation in the currently slipping region. Based on his mathematical results, the shear stress fluctuation vanishes when the propagation velocity reaches a specific value called the generalized Rayleigh wave speed, which is slightly lower than the S-wave speed of the more compliant medium, and the sign of the normal stress fluctuation depends on the propagation direction. The slipping region is unclamped for propagation in the positive direction and the region is clamped in the opposite case. On this basis, Weertman [1980] speculated that the slipping region propagates only at the generalized Rayleigh wave speed. On a frictional interface whose initial friction is above the initial shear stress level and where the coefficient of dynamic friction is constant, slipping regions can be kept in motion only in the positive direction because of self-unclamping; they cannot be moved in the negative direction because of self-clamping and lack of shear stress increment. The assumptions that the coefficient of dynamic friction is constant and that the propagation speed is at the generalized Rayleigh wave speed are too restrictive to apply to fault dynamics; in addition, such assumptions are not necessarily consistent with recent theoretical findings. Indeed, for the first assumption, Adams [1995] and Ranjith & Rice [2001] demonstrated that slippage on a bimaterial interface with a constant coefficient of dynamic friction is often unstable and ill-posed for a wide range of material parameters and friction coefficients. In principle, friction should vary from its maximum level to its dynamic level continuously. As for the latter assumption, in general, arbitrary propagation velocity should be considered because, in many cases, rupture velocities are seismologically estimated within a wide sub-Rayleigh range.

Following the studies of Weertman [1980] and Heaton [1990], many researchers have numerically investigated slip pulses propagating along a bimaterial interface [e.g., Andrews & Ben-Zion 1997; Ben-Zion & Andrews 1998; Cochard & Rice 2000; Shi & Ben-Zion 2006; Rubin & Ampuero 2007]. Their motivations were enumerated in the introduction of Ben-Zion & Andrews [1998]. A self-sustaining slip pulse propagating along a bimaterial interface with a constant coefficient of dynamic friction was simulated in the numerical analyses of Andrews & Ben-Zion [1997] and Ben-Zion & Andrews [1998]. However, Cochard & Rice [2000] showed that the numerical solutions of Andrews & Ben-Zion [1997] and Ben-Zion & Andrews [1998] are inherently unstable and diverge with an increasing number of grids. To stabilize the solutions, Cochard & Rice [2000] employed a friction that follows the change of normal stress with some relaxation time proposed on the basis of laboratory experiments [Prakash & Clifton 1993; Prakash 1998]; this is generally referred to as Prakash & Clifton's friction law. As a result, Cochard & Rice [2000] obtained a numerical solution for a self-sustaining slip pulse propagating only along the positive direction with a velocity 97% of the generalized Rayleigh wave speed. We should note that the friction law they employed is a function of the rate of shear stress change and is completely different from the slip-weakening friction laws that are used widely. Moreover, in an analytical treatment of Adda-Bedia & Ben Amar [2003], a slip pulse modeled with Prakash & Clifton's friction law was found to have unbounded slip velocity and normal stress; consequently, a physically reasonable analytic solution has not been obtained under the conditions employed by Cochard & Rice [2000] even from the point of view of an asymptotic analysis. In other words, it is still unclear whether Prakash & Clifton's law is reasonable for the slip pulse problem. Meanwhile, a numerical solution for a slip pulse propagating along a bimaterial interface has also been obtained on the assumption of a slip-weakening friction law [Shi & Ben-Zion 2006; Dalguar & Day 2009] or a friction law that has the dual nature of both slip-weakening and rate-weakening [Ampuero & Ben-Zion 2008]. Under these two friction laws, although only the pulse propagating along the positive direction tends to appear for a wide range of parameters, the pulse propagating along the negative direction can also appear for some parameter values. There is, however, no analytical treatment of pulses for these two friction laws. An analytical treatment should be performed using physically plausible conditions, including boundedness of stresses, to investigate precisely the dependence of slip behavior on many model parameters.

In the present paper, we model a steady-state slip pulse propagating along a bimaterial interface with three physically plausible conditions: arbitrary propagation speeds in the sub-Rayleigh range, a slip-weakening friction law, and boundedness of stresses. By following the methodology of Rice et al. [2005] and using the solution of Tricomi [1957], we find an analytical solution for the pulse. The analytical solution enables us to investigate precisely the dependence of the pulse on model parameters including the stress ratio S, slip-weakening distance, propagation direction, and propagation speed. On the basis of the analytical solution, we discuss conditions for the existence of a solution, the limitation of propagation speed, and suggestions for observational studies.

2. Modeling and solution

2.1. Modeling of a slip pulse

We construct an integral equation to represent the relation between stress and a steady-state mode II slip pulse on a bimaterial interface. This model, along with the method shown in the next subsection, can be regarded as a

generalization and mathematical refinement of the methodology of Rice et al. [2005]. A fault is assumed to lie along a frictional interface $Y = 0$ between two dissimilar isotropic, homogeneous, elastic, semi-infinite half-spaces. The P-wave and S-wave velocities are given by α and β, respectively, and ρ denotes the material density. The superscript $+$ denotes the medium above the interface ($Y > 0$) and $-$ the medium below ($Y < 0$). Across the fault, shear stress is defined as positive in right-lateral and normal stress is defined as positive in tension. By considering a rupture front along the fault moving in the negative direction of the X axis with a constant speed c ($< \min\{\beta^{\pm}\}$), and considering a steady-state distribution of slip $\Delta u(X,t) = \Delta u(X + ct)$, we can apply the Galilean transformation:

$$x := X + ct, \tag{1}$$

$$y := Y, \tag{2}$$

$$\frac{1}{c}\frac{\partial}{\partial t} = \frac{\partial}{\partial X} = \frac{\partial}{\partial x}, \tag{3}$$

where t is time. By employing this transformation, slip velocity $\Delta\dot{u}(x)$ (≥ 0) can be replaced by the slip gradient $\Delta u'(x)$. Using these notations, Weertman [1980] showed that shear stress $\tau(x)$ and normal stress $\sigma(x)$ along the fault are represented as follows:

$$\tau(x) = \tau_0 - \bar{\mu}\, p.v. \int \frac{\Delta u'(\xi)}{\xi - x}\frac{d\xi}{\pi}, \tag{4}$$

$$\sigma(x) = \sigma_0 + \mu^* \Delta u'(x), \tag{5}$$

where τ_0 (> 0) and σ_0 (< 0) are the initial shear and normal stresses, respectively, and $p.v.$ indicates Cauchy's principal value. The coefficients $\bar{\mu}$ and μ^* are functions of material parameters and the propagation speed. If the upper and lower materials are identical, we have the relation $\mu^* = 0$. The speed c_{GR} that satisfies the equation $\bar{\mu}(c_{GR}) = 0$ is referred to as the generalized Rayleigh wave speed. Although expressions for $\bar{\mu}$ and μ^* were given explicitly by Weertman [1980], the expression for μ^* contains a typographical error and was corrected by Cochard & Rice [2000]. For a Poisson solid, $|\mu^*|$ is an increasing and finite function of c, and μ^* is positive if $\alpha^+ < \alpha^-$ and $\beta^+ < \beta^-$, and is negative if $\alpha^+ > \alpha^-$ and $\beta^+ > \beta^-$. As we have fixed the propagation direction as the direction of $x = -\infty$, the former is the case of the positive direction, i.e., the self-unclamping case, and the latter is the case of the negative direction, i.e., the self-clamping case.

As we treat a slip pulse, the support of $\Delta u'$ is finite and is located only behind the rupture front. We situate the leading edge of the pulse, i.e., the rupture front, at $x = -1$ and the trailing edge of the pulse at $x = +1$ so that the interval of the integral in the RHS of eq. (4) is $(-1, +1)$. We assume that $\Delta u'$ is continuous and piecewise differentiable at $\forall x \in (-\infty, +\infty)$, which includes the relation $\lim_{\epsilon\to+0} \Delta u'(\pm 1 \mp \epsilon) = 0$. This is because the boundedness of stress, which is mentioned as one of the physically plausible conditions to be imposed in our model, is guaranteed by this continuity and differentiability (see Appendix A). We introduce the spatial variation of the coefficient of friction $f(x)$; this is a generalization of the approach of Rice et al. [2005]. As we assume that the slip velocity $\Delta\dot{u} = c\Delta u'$ is non-negative, the slip $\Delta u(x) = \int_{-1}^{x} \Delta u'(\xi) d\xi$ is a monotonically increasing function of x. Hence, the friction f must be a monotonically decreasing function of x in order to be slip-weakening. We define the coefficient of maximum static friction $f_s = \max f = f(-1)$ and the coefficient of dynamic friction $f_d = \min f = f(+1)$.

On the basis of these formulations, we can equate the shear stress and the friction on the slipping part of the plane

$Y = 0$;

$$\tau(x) + f(x)\,\sigma(x) = 0. \tag{6}$$

For convenience in later calculations, we rewrite f as follows:

$$f(x) = f_d + (f_s - f_d)\,F(x), \tag{7}$$

where F is a normalized monotonically decreasing function that satisfies $F(-1) = 1$ and $F(+1) = 0$. We thus obtain a singular integral equation of the Carleman type:

$$f(x)\Delta u'(x) - \lambda\, p.v. \int_{-1}^{+1} \frac{\Delta u'(\xi)}{\xi - x}\frac{d\xi}{\pi} = p + qF(x), \tag{8}$$

where $\lambda = \bar{\mu}/\mu^*$, $p = -(\tau_0 + f_d\,\sigma_0)/\mu^*$, and $q = -(f_s - f_d)\,\sigma_0/\mu^*$. We note that λ is positive if the pulse propagates along the positive direction and negative in the opposite case.

2.2. Analytical solution of the slip pulse with physically plausible conditions

An analytical solution of eq. (8) has been derived by Tricomi [1957] as

$$\Delta u'(x) = \frac{\{p + qF(x)\}\,f(x)}{f^2(x) + \lambda^2} + \lambda A(X)\, p.v. \int_{-1}^{+1} \frac{A^*(\xi)\,\{p + qF(\xi)\}}{\xi - x}\frac{d\xi}{\pi}, \tag{9}$$

where

$$A(x) = \frac{1}{\sqrt{f^2(x) + \lambda^2}}\left(\frac{1-x}{1+x}\right)^{\theta(x)/\pi} \exp\left\{p.v. \int_{-1}^{+1} \frac{\theta(\xi) - \theta(x)}{\xi - x}\frac{d\xi}{\pi}\right\}, \tag{10}$$

$$\theta(x) = \arctan\frac{\lambda}{f(x)} = \frac{\pi}{4} - \arctan\frac{f(x)}{\lambda}, \quad (0 < \theta < \pi), \tag{11}$$

$$A^*(x) = \frac{1}{\{f^2(x) + \lambda^2\}\,A(x)}. \tag{12}$$

Although Tricomi [1957] did not impose a specific condition for f, which was expressed as a in his book, the solution (9) is valid as long as the function a is bounded; see eq. (4) of Chapter 4.4 of his book for further details. We assume that our function f is piecewise smooth and that f' is bounded, i.e., f is Lipschitz continuous. This assumption guarantees the existence of Cauchy's principal values appearing in eqs. (9) and (10); note that θ also becomes Lipschitz continuous on the basis of its definition.

The solution (9) already satisfies two of the physically plausible conditions, that is, rupture speed in the sub-Rayleigh range and slip-weakening friction. Thus, the remaining problem is the continuity of $\Delta u'$. The relationship

$$\lambda\, p.v. \int_{-1}^{+1} \frac{A^*(\xi)}{\xi - x}\frac{d\xi}{\pi} = \mathrm{sgn}(\lambda) - f(x)A^*(x), \tag{13}$$

which was given as eq. (28) of the Chapter 4.4 in Tricomi [1957], helps in our calculation. After some algebra on eq. (9) and (13), we obtain the following:

$$\Delta u'(x) = \frac{\tau_p - \tau_r}{\bar{\mu}}\left\{\frac{1}{1+S} + F(x) + |\lambda|\ p.v. \int_{-1}^{+1} \frac{A^*(\xi)\,\{F(\xi) - F(x)\}}{\xi - x}\frac{d\xi}{\pi}\right\}|\lambda|\,A(x), \tag{14}$$

where $\tau_p = f_s\,|\sigma_0|$ is the yielding stress at the leading edge of the pulse, $\tau_r = f_d\,|\sigma_0|$ is the dynamic friction at the trailing edge of the pulse, and

$$S = \frac{\tau_p - \tau_0}{\tau_0 - \tau_r} \tag{15}$$

is the stress ratio mentioned in the introduction.

As F is assumed to be Lipschitz continuous, the integrand is bounded for $\forall x \in (-1, +1)$; therefore we no longer have to consider Cauchy's principal value of the integral. Moreover, the improper integral

$$\int_{-1}^{+1} \frac{A^*(\xi)\{F(\xi) - F(x)\}}{\xi - x}\frac{d\xi}{\pi} \tag{16}$$

exists for $\forall x \in [-1, +1]$ because an asymptotic form of A^* in the vicinity of both ends of the integration interval

$$A^*(\xi) \sim (1 \pm \xi)^{\mp\theta(\xi)/\pi}, \quad (\xi \sim \pm 1) \tag{17}$$

is integrable and, therefore,

$$\left|\int_{-1}^{+1} \frac{A^*(\xi)\{F(\xi) - F(x)\}}{\xi - x}\frac{d\xi}{\pi}\right| < K\int_{-1}^{+1} A^*(\xi)\frac{d\xi}{\pi} < +\infty \tag{18}$$

holds for $\forall x \in [-1, +1]$, where K is the Lipschitz constant for F. With this result and the definition of A, we find $\Delta u'(+1) = 0$.

Now only the condition $\lim_{\epsilon\to+0} \Delta u'(-1+\epsilon) = 0$ is our concern because $\Delta u'$ is clearly continuous for $\forall x \in (-1, +1]$ owing to the boundedness of the integrand of the improper integral (16) and the definition of A. Moreover, the existence of (16) at $x = -1$ and the Lipschitz continuity of F yield

$$\left\{-\frac{1}{1+S} + F(x) + |\lambda|\int_{-1}^{+1} \frac{A^*(\xi)\{F(\xi) - F(x)\}}{\xi - x}\frac{d\xi}{\pi}\right\} \sim C + K(1 + x) \tag{19}$$

in the vicinity of $x = -1$, where

$$C = -\frac{1}{1+S} + 1 + |\lambda|\int_{-1}^{+1} \frac{A^*(\xi)\{F(\xi) - 1\}}{\xi + 1}\frac{d\xi}{\pi} \tag{20}$$

is obtained as a limit of the LHS of eq. (19) at $x \to -1$. Hence, by taking into account the asymptotic form of A, the RHS of eq. (14) has an asymptotic form of

$$C'\{C + K(1 + x)\}(1 + x)^{-\theta(-1)/\pi} \tag{21}$$

in the vicinity of $x = -1$, where C' is a constant, and this approaches zero iff $C = 0$ by taking the limit $x \downarrow -1$ because $-1 < -\theta(-1)/\pi$ holds; otherwise this diverges owing to the singularity of A at $x = -1$. Thus we finally obtain the following equation for $\lim_{\epsilon\to+0} \Delta u'(-1 + \epsilon) = 0$:

$$-\frac{1}{1+S} + 1 + |\lambda|\int_{-1}^{+1} \frac{A^*(\xi)\{F(\xi) - 1\}}{\xi + 1}\frac{d\xi}{\pi} = 0. \tag{22}$$

The LHS of eq. (22) is a functional of F and contains S, f_s, f_d and λ as parameters. If both materials are identical, we obtain

$$|\lambda| A^*(\xi) = \sqrt{\frac{1+x}{1-x}}, \tag{23}$$

by taking $|\lambda| \to \infty$. Hence, for a homogeneous medium, the condition (22) does not contain f_s, f_d, or c as parameters, which means that S is determined uniquely once F is given, as already shown by Rice et al. [2005]. Our results, however, indicate that the condition of boundedness of stress depends on these parameters in the case of a bimaterial interface. We investigate this dependence in the next section.

Numerical evaluation of the improper integral (16) is achieved with difficulty by using Newton-Cotes formulae, including the trapezoidal rule and Simpson's rule, owing to the singularity of the integrand. It is, however, rapidly calculable by using the double exponential formula, which has been proved mathematically to be the best formula for numerical integrals [Takahashi & Mori 1974]. Hence, by using this formula, we calculate the condition (22), the integral appearing in the RHS of eq. (10) and, finally, the solution (14).

3. Analysis

3.1. Parameter ranges

We assume values of the parameters contained in the solution (14) as follows. For Poisson solids, $\alpha^+/\alpha^- = \beta^+/\beta^-$ holds. Moreover, we assume that $\rho^+/\rho^- = \alpha^+/\alpha^- = \beta^+/\beta^-$ holds approximately because $\alpha^+/\alpha^- \sim \rho^+/\rho^-$ for typical crustal rocks within an error of 10% [Birch 1961; Hirano & Yamashita 2011]. For the San Andreas fault system, the contrast of seismic wave velocities across faults lies between 5 and 30% [Shi & Ben-Zion 2006]. Below, we set $\beta^+/\beta^- = 1.2$ for rupture along the positive direction and $\beta^-/\beta^+ = 1.2$ for rupture along the negative direction. These values have been employed in previous numerical studies [Andrews & Ben-Zion 1997; Cochard & Rice 2000].

Rupture velocities of most earthquakes, except for deep earthquakes or tsunami earthquakes, are higher than 70% of the S-wave speed [Geller 1976; Venkataraman & Kanamori 2004], so we consider rupture velocities of 70 to 95% of the generalized Rayleigh wave speed in this section and of 95 to 100% of this speed in the next section.

We assume $f_s = 0.6, f_d = 0.2$, and a monotonically decreasing function F. Rice et al. [2005] treated a linear distance-weakening function:

$$F(x) = \begin{cases} -\frac{x+1}{2R} + 1 & (-1 < x < -1 + 2R) \\ 0 & (-1 + 2R < x < +1). \end{cases} \tag{24}$$

Although this function has only one parameter, R, the integral (16) has to be divided into two parts for numerical integration because it is not differentiable at $x = -1 + 2R$. To simplify the numerical integration procedure, we employ a smooth function

$$F(x) = \left(\frac{1-x}{2}\right)^{\frac{4}{R}-1}, \tag{25}$$

which is shown in fig.1-a and has the same L^1 norm as (24). We find that the relation between the stress ratio S and the process zone size obtained by substituting eq. (24) into (22) is almost the same as that obtained by substituting eq. (25) into (22) as shown in fig.1-b. This indicates that the difference between eq. (24) and eq. (25) is not significant.

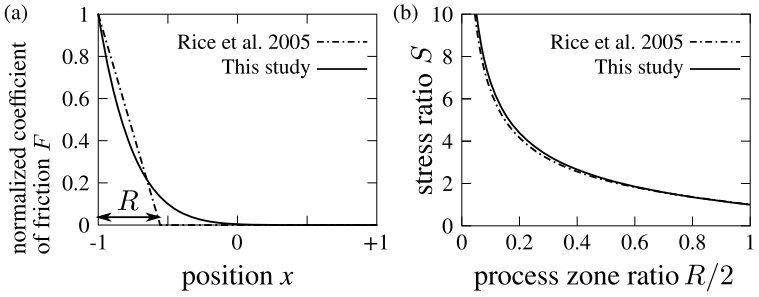

Figure 1: (a) Distributions of the normalized coefficient of friction F as a function of position x given by Rice et al. [2005] (dash-dot line) and this study (solid line). (b) Theoretical relationships between the stress ratio S and the process zone size R to satisfy eq. (22) for two friction distributions shown in (a).

3.2. Parameter dependence

First, the relationship between the stress ratio S and process zone size R given by eq.(22) is plotted in fig.2. This result shows that the relationship that fulfills the three physically plausible conditions introduced in the introduction depends on the direction and speed of rupture propagation for the bimaterial slip pulse whereas it does not depend on these factors in the homogeneous case. For any fixed value of S, the size of the process zone is smaller than that for the homogeneous model when the pulse propagates in the positive direction and is larger when the pulse propagates in the negative direction. For a pulse propagating in the negative direction, the curves never reach the level $S = 1$. This means that the pulse propagating in the negative direction cannot exist if $S \leq 1$. For $S > 1.5$ and $c/c_{GR} < 0,95$, however, the curves can reach any level of S. Hence, over a wide range of S, a pulse propagating in the negative direction can exist in the steady-state regime. This is a new insight, as such a possibility was not considered by Weertman [1980].

Next, distribution of slip velocity is plotted in fig.3. As for peak slip velocity, we find that its location depends mainly on S and its value depends mainly on c/c_{GR}. Moreover, both the location and value of peak slip velocity depend on the direction of pulse propagation. In addition, slip velocity peaks are observed near the leading edge of the pulse irrespective of its propagation direction; however, the peak is generally higher for a pulse propagating in the positive direction. This is likely to be an effect of the bimaterial interface.

Finally, dependence of slip-stress curves on propagation direction and velocity are plotted in fig.4. The result shows that slip-weakening distance becomes shorter as the rupture propagation velocity increases in the positive direction and becomes longer as the rupture propagation velocity increases in the negative direction. This occurs because the normal stress and process zone size depend on the direction and speed of rupture propagation.

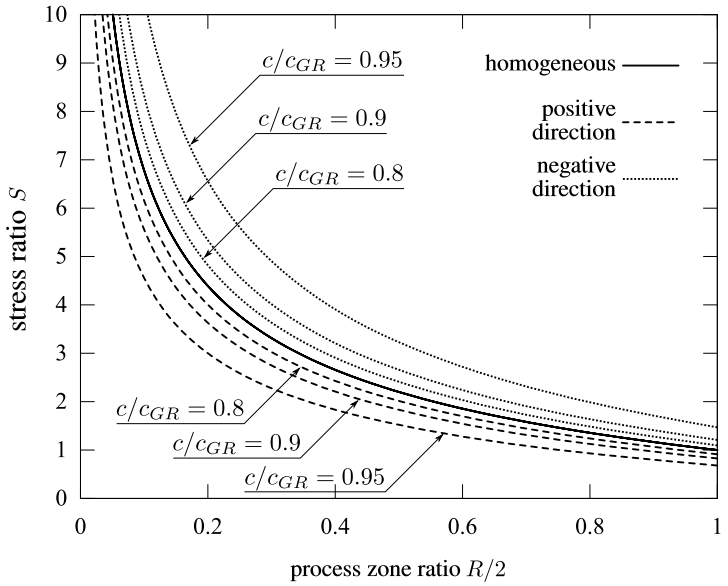

Figure 2: Relationships between the stress ratio S and process zone size R given by eq. (22). Solid line is the same as the solid line shown in fig.1-b and independent of rupture velocity. Dashed and dotted lines indicate that of the pulse propagating towards positive and negative directions of the bimaterial interface, respectively. For bimaterial cases, rupture velocities normalized by generalized Rayleigh wave speed c/c_{GR} are assumed to be 0.8, 0.9 and 0.95.

4. Discussion

4.1. Upper limit of rupture velocity

Weertman [1980] considered the possibility of self-sustained rupture propagation along a frictional bimaterial interface and concluded that the rupture can propagate only in the positive direction. In his study, he considered only the case of $c/c_{GR} = 1$ ($\bar{\mu} = 0$ in his context). We, however, find that $c/c_{GR} = 1$ is impossible even for the case of rupture in the positive direction, and that there exist limit values of c/c_{GR} in both propagation directions in our model.

When the rupture propagates in the negative direction, the maximum value of c/c_{GR} for which the condition (22) is satisfied is smaller for smaller values of S. When $S = 1.2$, for example, fig.2 shows that the condition (22) is satisfied for $c/c_{GR} = 0.9$ but is not satisfied for $c/c_{GR} = 0.95$. Hence, the rupture velocity of a pulse propagating in the negative direction lies only in the range $c/c_{GR} < 1$ and the upper limit velocity is smaller for smaller values of S.

When the rupture propagates in the positive direction, its velocity is limited by another mechanism. Eqs.(3) and (5) yield the following:

$$\sigma(x) = \sigma_0 + \frac{\mu^*}{c}\Delta\dot{u}(x), \tag{26}$$

where, not only μ^*, but also the maximum value of $\Delta\dot{u}$ are functions of the rupture velocity c according to fig.3. We plot the distribution of values of $\sigma(x)/\sigma_0$ for $c \sim c_{GR}$ in fig.5 and find that the normal stress becomes positive

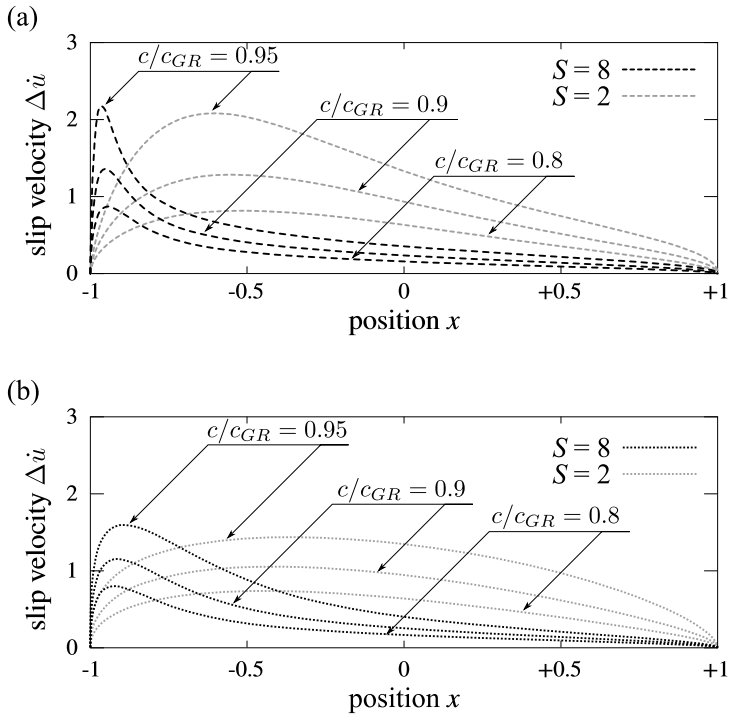

Figure 3: Slip velocity distributions inside of the pulse propagating towards (a) positive direction and (b) negative direction. Black and gray lines are for $S = 8$ and $S = 2$, respectively.

when $c/c_{GR} = 0.985$. For this tensile state, however, the friction law (6) is inappropriate and our model is no longer applicable. Hence, $c/c_{GR} \sim 0.98$ can be considered as the upper limit of rupture velocity in this model and we must somehow modify the friction law by taking into account the opening of the interface for $c/c_{GR} > 0.98$.

4.2. Suggestion for D_c-estimation in observational and/or experimental studies

In fig.4, we find that the ratio of critical slip distance (referred to as D_c) to final slip amount (referred to as D_{Max}) changes dramatically with rupture direction and velocity. Here we discuss implications of this finding.

The value of D_c/D_{Max} has been estimated and discussed widely [e.g., Mikumo et al. 2003; Tinti et al. 2005; Cocco et al. 2009]. This value is important in view of energy partitioning during earthquakes because the energy partitioning is discussed using the radiation efficiency $\eta_R := E_R/(E_G + E_R)$, where E_G and E_R are fracture energy and radiated energy, respectively, and η_R depends on D_c/D_{Max} (Appendix B). In seismology, estimation of D_c has been done under a framework of elastodynamics after inverting slip history at each point along a fault. Mikumo et al. [2003] has suggested $D_c/D_{\mathrm{Max}} \sim 0.27 - 0.56$ on the basis of seismic inversion analysis of the 1995 Kobe earthquake and the 2000 Western-Tottori earthquake and a numerical simulation. The variance of D_c/D_{Max} in their results might be due to many factors, e.g., spatial inhomogeneity of faults, suitability of their numerical model, etc. Our results, however, imply that accurate estimation of D_c might not be achieved without verifying whether or not the fault

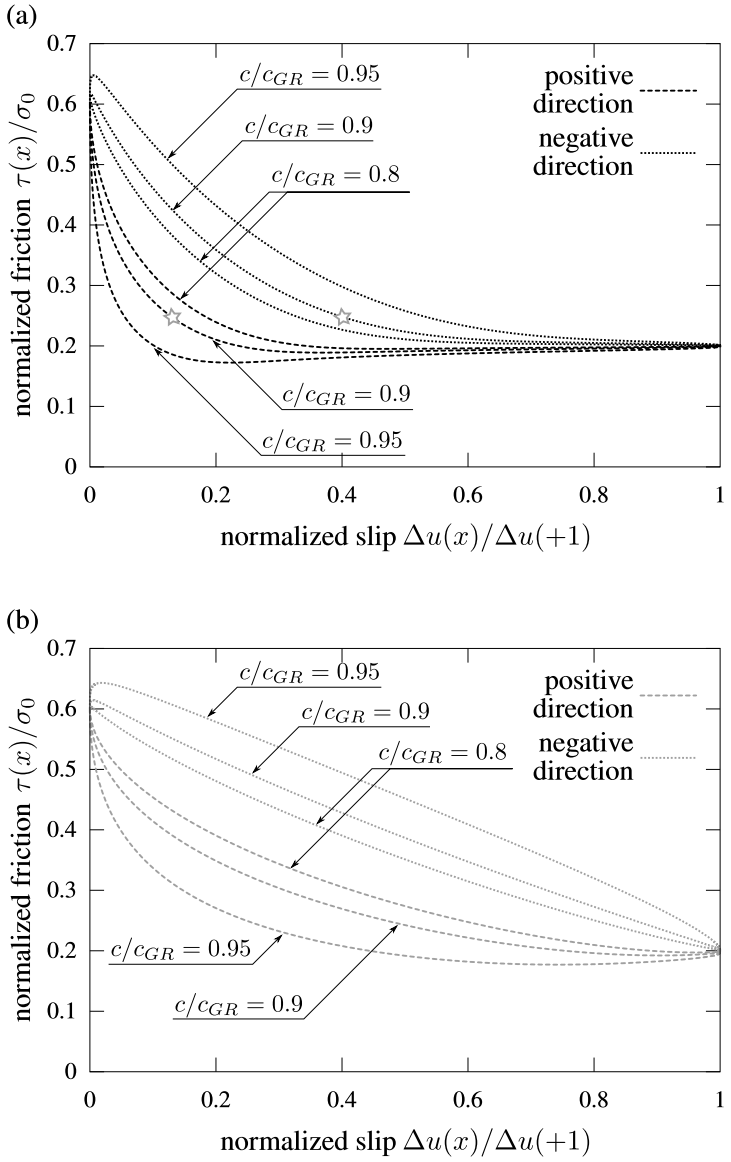

Figure 4: Slip-stress curves for (a) $S = 8$ and (b) $S = 2$. Dashed and dotted lines indicate that of the pulse propagating towards positive and negative directions, respectively. The abscissa is slip normalized by final slip $D_{\mathrm{Max}} = \Delta u(+1)$. Two stars for $S = 8$ indicate D_c for $c/c_{GR} = 0.9$, which is defined as the value of slip when the value of traction is 0.25.

lies on a bimaterial interface when converting the slip velocity profile to a slip-stress curve. Indeed, we find that $D_c/D_{\mathrm{Max}} \sim 0.1$ and ~ 0.4 for ruptures propagating in the positive and negative directions, respectively, for $S = 8$ and $c/c_{GR} = 0.9$ if, for simplicity, D_c is defined as the value of the normalized slip that gives 0.25 in traction (fig.4).

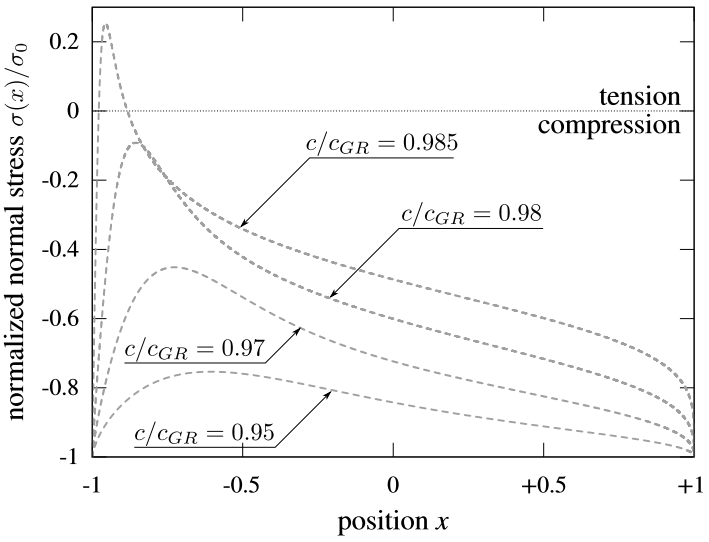

Figure 5: Normalized normal stress distribution $\sigma(x)/\sigma_0 = 1 + \mu^* \Delta\dot{u}(x)/(c\sigma_0)$ for the pulse propagating towards the positive direction when $S = 2$ and $c \sim c_{GR}$.

This means that rupture directivity can be clearly seen in the slip-stress curve rather than in the slip velocity profile; note that slip velocity profiles in fig.3 are not so different, even for $c/c_{GR} = 0.9$. Although material interfaces have not been considered in traditional schemes to estimate D_c from inversion analyses, we can conclude that the effect of the material interface on estimation is not negligible and suggest investigating the material contrast of both sides of a fault before conducting such analyses.

On the other hand, D_c can be estimated in laboratory experiments as the slip-weakening distance of friction between two rock masses. For interfacial faults, normal stress varies with slip and depends on the slip gradient as shown in eq.(5). Even if bimaterial interface is introduced in experimental settings, we will not be able to detect such slip gradient in traditional laboratory experiments because rock samples are usually too small to resolve the spatial distribution of friction or the slip gradient. Photoelastic experiments will be advantageous to obtain sufficient resolution of the slip gradient [Rosakis et al. 2007]. The singular integral equation (8) might be useful to estimate the constitutive law of friction in such experiments because eq.(8) tells us that $f = f\left(\Delta u'\right)$ can be obtained if $\Delta u'$ is given.

5. Summary

For an interfacial slip pulse propagating with constant velocity and length, we construct a Carleman-type singular integral equation (8) on the basis of Weertman's solution (4), (5), and the friction law (6). The friction coefficient $f(x)$ is a monotonically decreasing function of position; so $f(x)$ actually has a slip-weakening nature. Under physically plausible conditions of arbitrary sub-Rayleigh propagation speeds, a slip-weakening friction law, and boundedness of stress, we find an analytical solution (14) with (22). Eq.(22) gives a unique relationship between the stress ratio S,

the process zone size R, and the normalized rupture velocity c/c_{GR} while the relationship for a slip pulse propagating in a homogeneous medium that satisfies the three conditions does not depend on the rupture velocity as shown by Rice et al. [2005]. Moreover, our solution shows the directivity in distributions of slip velocity and slip-stress curves. One of our theoretical conclusions is that rupture velocity might be limited for ruptures in both the positive and negative directions; a range of existence of the solution limits the velocity in the negative direction and a range of negativeness of normal stress limits the velocity in the positive direction. Another important theoretical conclusion is that the characteristic slip-weakening distance D_c changes dramatically with the direction and velocity of rupture propagation. This suggests that estimation of D_c could be affected by the material interface and, therefore, that the material interface should be considered in observational studies.

Data and resources

No data were used in this paper. All plots were made using gnuplot version 4.6 patchlevel 4: http://www.gnuplot.info/.

Acknowledgements

We thank Satoshi Ide, Nobuki Kame and James R. Rice for useful discussions. We also appreciate helpful comments given by Luis A. Dalguer and two anonymous reviewers. This is a post-peer-review, pre-copyedit version of an article published in *Bull. Seism. Soc. Am.* The final authenticated version is available online at: https://doi.org/10.1785/0120150208.

References

Adams, G.G., 1995, Self-excited oscillations of two elastic half-spaces sliding with a constant coefficient of friction, *J. Appl. Mech.*, **62**, 867–872.

Adda-Bedia, M. & Ben Amar, M., 2003, Self-sustained slip pulses of finite size between dissimilar materials, *J. Mech. Phys. Solids*, **51**, 1849–1861.

Ampuero, J.-P. & Ben-Zion, Y., 2008, Cracks, pulses and macroscopic asymmetry of dynamic rupture on a bimaterial interface with velocity-weakening friction *Geophys. J. Int.*, **173**, 674–692.

Andrews, D.J., 1976, Rupture velocity of plane strain shear cracks, *J. Geophys. Res.*, **81**, 5679–5687.

Andrews, D.J., & Ben-Zion, Y., 1997, Wrinkle-like slip pulse on a fault between different materials, *J. Geophys. Res.*, **102**, 553–571.

Ben-Zion, Y. & Andrews, D.J., 1998, Properties and implications of dynamic rupture along a material interface, *Bull. Seism. Soc. Am.*, **88**(4), 1085–1094.

Birch, F., 1961, The velocity of compressional waves in rocks to 10 kilobars, Part 2, *J. Geophys. Res.*, **66**(7), 2199–2224.

Cocco, M., Tinti, E., Marone, C. & Piatanesi, A., 2009, Scaling of slip weakening distance with final slip during dynamic earthquake rupture, in: *Fault-Zone Properties and Earthquake Rupture Dynamics*, edited by Fukuyama, E., International Geophysics Series, 94, 163-186, Elsevier.

Cochard, A. & Rice, J.R., 2000, Fault rupture between dissimilar materials: Ill-posedness, regularization and slip-pulse response, *J. Geophys. Res.*, **105**, 25,891–25,907.

Dalguer, L.A. & Day, S.M., 2009, Asymmetric rupture of large aspect-ratio faults at bimaterial interface in 3D. *Geophys. Res. Lett.*, **36**, L23307.

Day, S.M., 1982, Three-dimensional finite difference simulation of fault dynamics: Rectangular faults with fixed rupture velocity, *Bull. Seism. Soc. Am.*, **72**(3), 705–727.

Garagash, D.I., 2012, Seismic and aseismic slip pulses driven by thermal pressurization of pore fluid, *J. Geophys. Res.*, **117**, B04314.

Geller, R.J., 1976, Scaling relations for earthquake source parameters and magnitudes, *Bull. Seism. Soc. Am.*, **66**, No. 5, pp. 1501–1523.

Heaton. T.H., 1990, Evidence for and implications of self-healing pulses of slip in earthquake rupture, *Phys. Earth Planet. Int.*, **64**, 1–20.

Hirano, S., & Yamashita, T., 2011, Analysis of the static stress field around faults lying along and intersecting a bimaterial interface, *Geophys. J. Int.*, **187**(3), 1460–1478.

Ishii, M., Shearer, P.M., Houston, H. & Vidale, J.E., 2005, Extent, duration and speed of the 2004 Sumatra-Andaman earthquake imaged by the Hi-Net array, *Nature*, **435**, 933–936.

Mikumo, T., Olsen, K.B., Fukuyama, E. & Yagi, Y., 2003, Stress-breakdown time and slip-weakening distance inferred from slip-velocity functions on earthquake faults, *Bull. Seism. Soc. Am.*, **93**, No. 1, pp. 264–282.

Nakamura, H. & Miyatake, T., 2000, An approximate expression of slip velocity time function for simulation of near-field strong ground motion (in Japanese with English abstract), *Zisin* (*J. Seism. Soc. Japan.*) II. **53**(1), 1–9.

Nielsen, S., & Madariaga, R., 2003, On the self-healing fracture mode, *Bull. Seism. Soc. Am.*, **93**(6), 2375–2388.

Noda, H., Dunham, E.M., & Rice, J.R., 2009, Earthquake ruptures with thermal weakening and the operation of major faults at low overall stress levels, *J. Geophys. Res.*, **114**, B07302.

Okuwaki, R., Yagi, Y. and Hirano, S., 2014, Relationship between high-frequency radiation and asperity ruptures, revealed by hybrid back-projection with a non-planar fault model, *Sci. Rep.*, **4**:7120.

Prakash, V & Clifton, R.J., 1993, Time resolved dynamic friction measurements in pressure-shear, in: *Experimental techniques in the dynamics of deformable solids*, edited by A. K. T. Ramesh, pp. 33–48, Appl. Mech. Div., Am. Soc. of Mech. Eng., New York.

Prakash, V., 1998, Frictional response of sliding interfaces subjected to time varying normal pressures, *J. Tribol.*, **120**, 97–102.

Ranjith, K. & Rice, J.R., 2001, Slip dynamics at an interface between dissimilar materials, *J. Mech. Phys. Solids*, **49**, 341–361.

Rice, J.R., Sammis, C.G. & Parsons, R., 2005, Off-fault secondary failure induced by a dynamic slip pulse, *Bull. Seism. Soc. Am.*, **95**(1), 109–134.

Rubin, A.M., & Ampuero, J.-P., 2007, Aftershock asymmetry on a bimaterial interface, *J. Geophys. Res.*, **112**, B05307.

Shi, Z., & Ben-Zion, Y., 2006, Dynamic rupture on a bimaterial interface governed by slip-weakening friction, *Geophys. J. Int.*, **165**, 469–484.

Suzuki, T., & Yamashita, T., 2008, Nonlinear effects of temperature, fluid pressure, and inelastic porosity on dynamic fault slip and fault tip propagation: Emergence of slip strengthening and pulse-like fault slip, *J. Geophys. Res.*, **113**, B07304.

Takahashi, H., & Mori, M., 1974, Double exponential formulas for numerical integration, *Publ. RIMS, Kyoto Univ.*, **9**, 721–741.

Tinti, E., Fukuyama, E., Piatanesi, A. & Cocco, M., 2005, A kinematic source-time function compatible with earthquake dynamics, *Bull. Seism. Soc. Am.*, **95**(4), 1211–1223.

Tricomi, F.G., 1957, *Integral equations*, New York: Dover.

Venkataraman. A & Kanamori, H., 2004 , Observational constraints on the fracture energy of subduction zone earthquakes, *J. Geophys. Res.*, **109**, B05302.

Weertman, J.J., 1963, Dislocations moving uniformly on the interface between isotropic media of different elastic properties, *J. Mech. Phys. Solids*, **11**, pp. 197–204.

Weertman, J.J., 1969, Dislocation motion on an interface with friction that is dependent on sliding velocity, *J. Geophys. Res.*, **74**(27), 6617–6622.

Weertman, J.J., 1980, Unstable slippage across a fault that separates elastic media of different elastic constants, *J. Geophys. Res.*, **85**, 1455–1461.

Zheng, G., & Rice, J.R., 1998, Conditions under which velocity-weakening friction allows a self-healing versus a cracklike mode of rupture, *Bull. Seism. Soc. Am.*, **88**(6), 1466–1483.

Appendix A. Boundedness of stress

We show here that the boundedness of stress is guaranteed if the slip velocity $\Delta\dot{u} = c\Delta u'$ is continuous and piecewise differentiable at $\forall x \in (-\infty, +\infty)$. If $\Delta u'$ is continuous, Cauchy's principal value appearing in eq. (4) can be divided into the following three terms:

$$\begin{aligned}
p.v. \int_{-\infty}^{+\infty} \frac{\Delta u'(\xi)}{\xi - x} \frac{d\xi}{\pi} &= \lim_{\epsilon \to +0} \left\{ \int_{-\infty}^{x-\epsilon} + \int_{x+\epsilon}^{-\infty} \right\} \frac{\Delta u'(\xi)}{\xi - x} \frac{d\xi}{\pi} \\
&= \lim_{\epsilon \to +0} \left\{ \int_{-\infty}^{x-\epsilon} + \int_{x+\epsilon}^{-\infty} \right\} \left\{ \frac{\Delta u'(\xi) - \Delta u'(x) + \Delta u'(x)}{\xi - x} \right\} \frac{d\xi}{\pi} \\
&= \lim_{\epsilon \to +0} \int_{-\infty}^{x-\epsilon} \frac{\Delta u'(\xi) - \Delta u'(x)}{\xi - x} \frac{d\xi}{\pi} \qquad \text{(A.1)} \\
&\quad + \lim_{\epsilon \to +0} \int_{x+\epsilon}^{+\infty} \frac{\Delta u'(\xi) - \Delta u'(x)}{\xi - x} \frac{d\xi}{\pi} \qquad \text{(A.2)} \\
&\quad + \frac{\Delta u'(x)}{\pi} p.v. \int_{-\infty}^{+\infty} \frac{d\xi}{\xi - x}. \qquad \text{(A.3)}
\end{aligned}$$

In the one-sided limits of $\xi \to x \pm \epsilon$ and $\epsilon \to 0$, the integrands appearing in the terms (A.1) and (A.2) converge towards the left and right derivatives of $\Delta u'$, respectively, so that they are integrable even if one or both of the integrands diverge at x. Moreover, the term (A.3) is zero. Hence Cauchy's principal value of the LHS, which gives the shear stress change along the fault, exists (i.e., is bounded) for $\forall x \in (-\infty, +\infty)$. In particular, we assume that $\Delta u'$ is supported on $[-1, +1]$, so $\lim_{\epsilon \to +0} \Delta u' (\pm 1 \mp \epsilon) = 0$ holds.

On the other hand, Cauchy's principal value has a logarithmic singularity if $\Delta u'$ is bounded and discontinuous, and has a singularity of negative exponents if $\Delta u' \sim r^{-\alpha}$, where r is the distance from a discontinuous point of $\Delta u'$ and $0 < \alpha < 1$ [Adda-Bedia & Ben Amar 2003]. Therefore stress is bounded iff the slip velocity is continuous and piecewise differentiable.

Appendix B. Relation between $D_c/D_{\mathbf{Max}}$ and the radiation efficiency

We show how D_c/D_{Max} is significant for determination of the radiation efficiency defined as $\eta_R := E_R/(E_G + E_R)$ [Venkataraman & Kanamori 2004], which is widely used in discussion on energy partitioning of earthquakes. With the notations introduced in "Modeling of a slip pulse" section, we assume that the slip-stress relation can be approximated by the following function:

$$\tau(\Delta u) = \begin{cases} \tau_f(\Delta u / D_c), & \Delta u \le D_c, \\ \tau_d, & \Delta u > D_{\mathrm{Max}}, \end{cases} \qquad \text{(B.1)}$$

where an arbitrary continuous function τ_f satisfies $\tau_f(0) = -f_s\sigma_0$, which is the maximum static friction, and $\tau_f(1) = \tau_d = -f_d\sigma^0$, which is the dynamic friction. Under this assumption,

$$\begin{aligned} E_G &= \int_S dS \int_0^{D_{\mathrm{Max}}} \{\tau\,(\Delta u/D_c) - \tau_d\}\, d\Delta u \\ &= \langle D_c \rangle S \int_0^1 \{\tau_f(s) - \tau_d\}\, ds \end{aligned} \tag{B.2}$$

holds, where S indicates the entire fault surface and $\langle\,\cdot\,\rangle$ indicates average on S. Moreover,

$$E_G + E_R = \frac{\tau_0 - \tau_d}{2} \langle D_{\mathrm{Max}} \rangle S \tag{B.3}$$

holds [Venkataraman & Kanamori 2004]. Eqs.(B.2) and (B.3) result in

$$\begin{aligned} \eta_R &= 1 - \frac{E_G}{E_G + E_R} \\ &= 1 - \frac{2}{\tau_0 - \tau_d} \frac{\langle D_c \rangle}{\langle D_{\mathrm{Max}} \rangle} \int_0^1 \{\tau_f(s) - \tau_d\}\, ds. \end{aligned} \tag{B.4}$$

Therefore, the radiation efficiency depends on $\langle D_c \rangle / \langle D_{\mathrm{Max}} \rangle$.